Multi-Tone Transmission for Asymmetric Digital Subscriber Lines (ADSL)

Kamran Sistanizadeh (Bellcore), Peter S. Chow (Stanford University), and John M. Cioffi (Amati Corporation)

Bellcore
MRE-2K-250, 445 South Street, Morristown, NJ 07960-1910.
Tel: (201)-829-5130, Fax: (201)-829-5976

ABSTRACT

Multi-Tone transmission is a potentially viable technique for application on Asymmetrical Digital Subscriber Lines (ADSL). This paper presents the results of a preliminary study on the performance of an ideal Discrete Multi-Tone (DMT) signaling technique for a 1.6 Mb/s ADSL. The performance margins using single-tone 16-point Quadrature Amplitude Modulation (QAM) with an ideal Decision Feedback Equalization (DFE) are also presented. The feedforward filter of the DFE is a quarter-baud spaced Fractionally Spaced Equalizer (FSE). The interference is assumed to be the sum of far-end crosstalk (FEXT) and additive white Gaussian noise (AWGN). The subscriber loops are assumed to be in a plant environment where the maximum resistance does not exceed 1300 ohms. The projected performance of an ideal DMT with a sampling rate of 1.024 MHz and 256-subchannel segmentation offers potential margin enhancement up to 3 dB over a quarter baud-spaced FSE-based 16-QAM signaling.

1. Introduction

Asymmetric Digital Subscriber Line (ADSL) is a digital transport technology that could provide high-bandwidth services on existing non-loaded subscriber loops. Although the data rate has not been established yet, the prevailing consensus is that initial ADSL system will transport 1.544 Mb/s from the network towards the customer on a single twisted-pair telephone line up to 18 kft. Thus, POTS and high rate services would be provided on the same loop.

ADSL is an access technology that is intended to serve residential customers, enabling such potential services as: VCR-quality video on demand, video browsing, information services, CD-quality music, interactive games, home shopping, and other multi-media applications. Non-residential applications might include computer-aided design, remotely conducted educational sessions, and database services.

Because of the asymmetric nature of the high-bandwidth service (from the CO to the customer), the loop plant characteristics, the noise environment, and the existence of analog POTS, the transmission technique and the transceiver architecture for ADSL will be distinctly different from predecessor Basic Rate DSL[1] and High-rate DSL (HDSL)[2] technologies.

Presently, there are three contending transmission technologies: Quadrature Amplitude Modulation (QAM),[3] Carrierless Amplitude/Phase modulation (CAP),[4] and the Discrete Multi-Tone (DMT)[5] technique. A comprehensive assessment of various trade-offs for each of these techniques is currently being carried out through ANSI-T1E1.4 Standards Committee deliberations.

This paper is a computer analysis of the performance margin of two of the transmission techniques: uncoded single-tone 16-point QAM and ideal DMT. The QAM receiver is based on an ideal Decision Feedback Equalization (DFE) with *finite length* feedforward Fractionally Spaced Equalizer (FSE). The interference is assumed to be the sum of far-end crosstalk (FEXT) and additive white Gaussian noise (AWGN). The test loops are extracted from the canonical loops[6] that are at the extreme range of the non-loaded loop plant.

Such issues as functionality, programmability, flexibility, and control channel implementation of DMT have been discussed by Cioffi, et al.[7] More elaborate results have also been presented on the performance of DMT in the presence of impulse noise.[8] The underlying theoretical analysis for DMT is delineated in a T1E1.4 Technical Contribution,[9] and the ideal DFE-based QAM transceiver is discussed by Sistanizadeh in a GLOBECOM'90 paper.[10]

For a Bit Error Rate (BER) of 10^{-7}, the performance margin of an uncoded DMT-based system can be computed from the knowledge of the overall system signal to noise ratio (SNR), the number of bits per block, and the number of used sub-channels (see Section 2, the Appendix, and Reference [9] for details).

For the uncoded QAM system, the performance index, defined by the average SNR at the detector output of the in-phase channel (with perfect post-cursor ISI cancellation), is calculated from:[10]

$$(SNR)_{I-opt} = \frac{\left[(\underline{R}_{II})^{\dagger}_{opt}\, \underline{\phi}_I + (\underline{R}_{QI})^{\dagger}_{opt}\, \underline{\psi}_I \right]^2}{\left[1 - (\underline{R}_{II})^{\dagger}_{opt}\, \underline{\phi}_I - (\underline{R}_{QI})^{\dagger}_{opt}\, \underline{\psi}_I \right]}$$

where subscripts (I) and (Q) refer to in-phase and quadrature-phase channels respectively, and ($\dagger$) denotes the transpose operation. The performance margin for a BER of 10^{-7} and a 16-QAM rectangular constellation can be approximated by:[11] $\Delta_{QAM-margin} = 10 \log_{10} (SNR)_{I-opt} - 21.5\ dB$.

The organization of this paper is as follows. Section 2 briefly describes the system principles and delineates the computational algorithm for the performance margin. Section 3 discusses the loop plant environment, FEXT model, QAM transceiver structure, and the DMT simulation parameters. Section 4 presents the computer analyses results. Section 5 is a summary of results. Finally, a derivation of the DMT margin expression is presented in the Appendix.

2. Discrete Multi-Tone (DMT) System

2.1 The System Principles

The underlying idea is to divide the channel spectrum into several sub-channels (i.e., frequency bands) and transmit and receive data separately in each sub-channel. This is generically depicted in Figure 1. The transmit spectrum for each sub-channel is assumed to have identical energy spectral density, as illustrated in Figure 2. The block diagram of the proposed transceiver is shown in Figure 3. The operation of the transceiver is described as follows.

The input bit stream at the rate of R bits/sec is buffered into blocks of $b_{DMT} = R\ T_{DMT}$ bits, where T_{DMT} denotes the *DMT symbol period*. The *DMT symbol rate* is denoted by $f_{symbol-DMT} \equiv \frac{1}{T_{DMT}}$. The buffered bits are shared by several sub-channels. The bit allocation strategy follows an optimization criterion based on the achievable signal to noise ratio such that: $b_{DMT} = \sum_{j=1}^{M} b_j$. Each of the b_j bits are mapped into a *complex*

0-7803-0950-2/93/$3.00©1993IEEE

DMT sub-symbol $X_{j,k}$, where j and k denote the sub-channel and the buffer time index respectively. The set of sub-symbols for each sub-channel forms the QAM constellation of that sub-channel. For a sub-channel with an allocated b_j bits, there should exist 2^{b_j} unique sub-symbols.

The IFFT maps the M complex sub-symbols into $2M$ real time domain samples $x_{i,k}$ (i = 1,2,...,2M). This set of $2M$ real samples constitute the *k-th DMT transmitted symbol*. These $x_{i,k}$'s are passed through a Parallel to Serial (P/S) device, and applied to a Digital to Analog Converter (DAC) with sampling rate of: $f_{sample-DMT} = \frac{2M}{T_{DMT}}$. The low-passed output of the DAC is the transmitted waveform $x(t)$ on the channel.

The channels of interest are the highly dispersive and lossy subscriber loops. When the number of sub-channels is sufficiently large, the channel transfer function, $H(f)$, can be approximated by a set of contiguous rectangular sub-channel transfer functions of width $\frac{1}{T_{DMT}} = \frac{f_{sample-DMT}}{2M}$ Hz and with center-frequency gain $|H(f_j)|^2$ (j=1,2,..,M). With such an approximation, the channel can be decomposed into a set of discrete-time, parallel, independent, ISI-free sub-channels with gains $|H(f_j)|^2$. It can be shown that with large M, the noise components on each sub-channel are independent if the noise is Gaussian.[12] Thus, each independent sub-channel can be decoded separately using a memoryless detector (i.e., without equalization).

The operation of the receiver proceeds as the reverse of the transmit operation: low-pass filtering of the received signal $y(t)$, analog to digital conversion, serial to parallel formation, FFT processing on the $2M$ samples, and buffering/decoding to generate data at the rate of R bits/sec.

The IFFT is an energy invariant orthogonal transformation. That is: $\sum_{j=1}^{M} |X_{j,k}|^2 = \sum_{i=1}^{2M} x_{i,k}^2$. The mean-squared value of the $X_{j,k}$ is called the *sub-symbol energy* and is denoted by E_j; thus, the *sub-symbol power* is defined by $P_j = \frac{E_j}{T_{DMT}}$. Therefore, the total transmit energy and power denoted by E_{trans} and P_{trans} can be expressed by:

$$P_{trans} = \frac{E_{trans}}{T_{DMT}} = \frac{\sum_{j=1}^{M} E_j}{T_{DMT}} = \sum_{j=1}^{M} P_j \qquad (1)$$

The energy per sub-channel can be related to the number of square QAM signal constellations by:

$$E_j = \frac{L-1}{6} d^2 \qquad (2)$$

where L is the number of symbols in the constellation, and d is the distance between two adjacent symbols in each dimension. For example, with 16-QAM rectangular constellation using 4 symbols in each dimension L=16 , d=2, and E_j = 10. For a sufficiently large M, the signal to noise ratio on each sub-channel can be written as:

$$SNR_{j,M-DMT} = \frac{E_j |H_j|^2}{\sigma^2_{j-Noise}} \qquad j = 1, \cdots, M \qquad (3)$$

The total number of bits that can be allocated to all the sub-channels is expressed as:

$$b_{DMT} = \sum_{j=1}^{M} b_j = \log_2 \left\{ \prod_{j=1}^{M} \left[1 + \frac{SNR_{j,M-DMT}}{\Gamma_{DMT}} \right] \right\} \qquad (4)$$

where, for a BER of 10^{-7}, the uncoded *SNR Gap*, Γ_{DMT}, is approximated[9] by:

$$\Gamma_{DMT} = 9.8dB + \Delta_{DMT-margin} \qquad (5)$$

An average DMT signal to noise ratio for the overall system can be defined by $\overline{SNR}_{DMT}$ such that:

$$b_{DMT} = M \log_2 \left[1 + \frac{\overline{SNR}_{M-DMT}}{\Gamma_{DMT}} \right] \qquad (6)$$

Thus:

$$\overline{SNR}_{M-DMT} = \Gamma_{DMT} \left\{ \left[\prod_{i=1}^{M} \left(1 + \frac{SNR_{i,M-DMT}}{\Gamma_{DMT}} \right) \right]^{\frac{1}{M}} - 1 \right\} \qquad (7)$$

Assuming that "+1" and "-1" are negligible, the average SNR can be written as:

$$\overline{SNR}_{M-DMT} = \left[\prod_{i=1}^{M} (SNR_{i,M-DMT}) \right]^{\frac{1}{M}} \qquad (8)$$

Then from equation (6), the margin can be calculated by:

$$\Delta_{DMT-margin} = 10\log_{10} \left[\frac{\overline{SNR}_{M-DMT}}{2^{\frac{b_{DMT}}{M}} - 1} \right] - 9.8 \qquad (9)$$

Equation (9) is used for performance evaluation study of the DMT system.

2.2 Computational Algorithm for Performance Margin

Equation (9) expresses achievable margin through the average channel signal to noise ratio ($\overline{SNR}_{M-DMT}$), the optimal number of used sub-channels (M), and the desired number of bits per block (b_{DMT}).

For a given channel, sampling rate, and the number of allowed sub-channels ($\bar{N}$), an $\bar{N} \times \bar{N}$ "*sorted sub-channel matrix*" can be computed as:

$$\begin{bmatrix} SNR_{1,1-DMT} & SNR_{2,1-DMT} & SNR_{3,1-DMT} & \cdots & SNR_{\bar{N},1-DMT} \\ SNR_{1,2-DMT} & SNR_{2,2-DMT} & SNR_{3,2-DMT} & \cdots & SNR_{\bar{N},2-DMT} \\ SNR_{1,3-DMT} & SNR_{2,3-DMT} & SNR_{3,3-DMT} & \cdots & SNR_{\bar{N},3-DMT} \\ \vdots & \vdots & \vdots & \cdots & \vdots \\ SNR_{1,(\bar{N}-1)-DMT} & SNR_{2,(\bar{N}-1)-DMT} & SNR_{3,(\bar{N}-1)-DMT} & \cdots & SNR_{(\bar{N}),(\bar{N}-1)-DMT} \\ SNR_{1,\bar{N}-DMT} & SNR_{2,\bar{N}-DMT} & SNR_{3,\bar{N}-DMT} & \cdots & SNR_{\bar{N},\bar{N}-DMT} \end{bmatrix} \qquad (10)$$

where the elements of each row are the signal to noise ratio for each of the $\bar{N}$ sub-channels listed in the descending order (i.e., $SNR_{k,M-DMT} > SNR_{k+1,M-DMT}$). The value of the used-subchannels corresponds to the row number (i.e., the first row corresponds to M=1, and the second row corresponds to M=2, etc). Note that the effects of bridged-taps or gauge changes on the subscriber loops is exhibited in this matrix by the variation of SNR with respect to the position of the center frequency of the sub-channels. That is, the SNR on a sub-channel is not necessarily a monotonically decreasing function of its center frequency (i.e., a higher center frequency might support a larger SNR than a lower center frequency).

The lower diagonal portion of the above matrix forms the "*used sub-channel matrix*", where the M-th row has M associated largest sub-channels. Next, equation (8) is applied to each row to calculate an average SNR for a given M. Finally, the optimal channel SNR is the maximum of the computed SNR:

$$\overline{SNR}_{M-DMT} = Maximum\left\{ \overline{SNR}_{1-DMT}, \overline{SNR}_{2-DMT}, \overline{SNR}_{3-DMT}, \cdots, \overline{SNR}_{(\bar{N}-1)-DMT}, \overline{SNR}_{\bar{N}-DMT} \right\}$$

The optimal number of sub-channels is M, the index associated with $\overline{SNR}_{M-DMT}$.

3. Computer Simulation Framework

3.1 Loop Plant Environment

A set of five loops from the 1983 Loop survey,[13] as shown in Figure 5, are used for simulation studies. These loops have also been proposed as test loops for performance studies of various ADSL transceiver architectures in T1E1.4 Standards Committee.[6] Each loop is identified by a number as depicted in the loop make-up diagram (to the left of the "CO" in the Figures). In the simulation studies, an extra set of three loops are added to the canonical loops: 12 kft of 24-AWG (loop #16), 18 kft of 24-AWG (loop #17), and 9 kft of 26-AWG (loop #18). These loops are quite lossy and dispersive. For example, at 70° F, the pulse height loss of 18-kft, 24-AWG is about 61 dB at a carrier frequency of 250 kHz with 16-QAM signaling.

3.2 FEXT and AWGN Models

The coupling path for the generation of FEXT is dependent on the loss characteristics of the disturbing loop and the loss coupling function according to:

$$\left| H_{FEXT}(f) \right|^2 = \left| H_{disturbing}(f,l) \right|^2 k\, l\, f^2$$

where $\left| H_{disturbing}(f,l) \right|$ is the magnitude of the disturbing loop loss function. The coupling constant k, for 1% equal level 49 disturber crosstalk, is assumed to be 8×10^{-20} (with l in feet and f in Hz), where l is the length of the coupling path. Since the focus of the present study is to evaluate the effects of FEXT and the additive white Gaussian noise, the effects of NEXT from other systems are not considered in this study.

The AWGN level is set at -140 dBm/Hz. This is equivalent to $\sigma^2_{AWGN} = 10^{-15}\ V^2$ per Hz across a 100-ohm termination, or 4×10^{-12} Watts across 400-kHz of bandwidth.

3.3 QAM ADSL Transceiver Structure

The single-tone QAM ADSL system uses 16-point QAM for signaling at a nominal rate of 1.6 Mb/s. This rate is 56 kb/s above 1.544 Mb/s and can accommodate sufficient overhead. The symbols are extracted from a rectangular constellation with 4 symbolic levels of ± 3, ± 1 on each dimension. The source and load impedances are assumed to be 100-ohm resistive at 70° F, with the resulting transmit power of 20 dBm at the source. The transmit and receive lowpass filters are 10-th order Butterworth with the 3-dB corner frequency at 200 kHz. The carrier frequency, f_c, is determined by: $f_c = f_{guardband} + f_{3-dB}$ where $f_{guardband}$ (i.e., the frequency band from DC to the lower 3-dB point of the bandpass filter) is a simulation parameter in the range of 20 to 110 kHz.

A detailed description of the simulated QAM receiver can be found in a previous paper by the author.[10] As illustrated in Figure 4, the in-phase, quadrature-phase, and cross-coupled feedforward filters (FFF), respectively denoted by R_{11}, R_{22}, R_{12}, and R_{21} are designed to minimize the sum of the pre-cursor ISI and the additive noise at the input to the slicer. The optimal tap weights of the FFFs are obtained through minimization of the mean-squared error (MSE) at the output of the FFFs (in the absence of post-cursor ISI). A quarter baud-spaced Fractionally Spaced Equalizer (FSE) is used for pre-cursor equalization. A 41-tap FSE is assumed for the feedforward and cross-coupled filters. The pulse response of each loop is assumed to have a span of 15 pre-cursor and 60 post-cursor bauds with respect to its cursor.

3.4 DMT Simulation Parameters

For DMT margin computation, the transmit power is also assumed to be 20 dBm at the source with 100-ohm terminations. It is assumed that the sampling rate is 1.024 MHz, and the channel is decomposable into 256 sub-channels. That is each sub-channel occupies 2 kHz of channel bandwidth. With such an arrangement, the maximum sub-channel center frequency is at 256×2 = 512 kHz. Thus, searching for optimum sub-channels is conducted at carrier frequencies of $f_i = 2\,i$ kHz for $i = 1, \cdots, N$=256. Furthermore, it is also assumed that the power is equally divided amongst the used sub-channels, and the discarded sub-channels do not have any energy. This is an important assumption since the resulting transmit spectrum will not be uniform across the channel bandwidth.

4. Computational Results

The results of the DMT margin computations are tabulated in Table 1 for the case where all sub-channels are allowed to be used (i.e., $f_i = 1, \cdots, 256$). Note that the computed DMT margin is sufficiently high even with loop #1. Table 2 tabulates the results of the margins for both 16-QAM and DMT for three values of guardbands: 20, 50, and 100 kHz. For the QAM study, the guardband refers to the lower 3-dB point of the band-pass filter that determines the region of channel spectrum usage. For the case of DMT with 2-kHz sub-channel bandwidth, 20, 50, and 100 kHz refer to excluding the first 10, 25, and 50 lower sub-channels from usage for bit distribution. This sub-channel exclusion scenario imposes a severe penalty on the performance of the DMT. However, since the inclusion of POTS and a "reverse control channel" has not been investigated, the sub-channel exclusion strategy as a preliminary simulation approach is deemed to be a judicious method for comparison with a QAM system.

The last three columns of Table 2 show the relative enhancement of an ideal DMT over 16-QAM. The tabulated results indicate that *generally*, for a given guardband, DMT has a higher margin than QAM across the loops. This enhancement is more evident at lower guardbands where only the first 10 sub-channels form the exclusion region. As the guardband increases, the flexibility of DMT in energy distribution weakens, and thus the relative advantage of DMT decreases.

It is instructive to remark on the following points:

1. A higher sampling rate is conjectured to improve the theoretical performance for certain loops.
2. In the DMT margin computations, the loop transfer function *did not* include any low-pass or band-pass filters associated with any segment of the system.
3. By excluding a number of sub-channels in the lower channel spectrum (i.e., utilizing a brickwall type exclusion region), some of the inherent advantages of DMT are discarded. That is, at the critical low frequency region where the channel gains are higher, the ability of DMT to vary the bit distribution is weakened.
4. The number of channel pre-cursors in the equalization of the QAM channel was set at 60 (i.e., 15 bauds with T/4-FSE), and the number of post-cursors was set at 240 (i.e., 60 bauds with T/4-FSE). The size of these two parameters are quite significant when the guardband is below 40 kHz.
5. It was observed that the so-called "Narrow-Band" channel model[11] for a QAM system is valid at guardbands above 40 kHz with 10-th order Butterworth filters. For guardbands below 40-kHz, four channel pulse responses should be computed: in-phase, quadrature-phase, and two cross-coupled channels (in-phase to quadrature-phase and quadrature-phase to in-phase).

5. Conclusions

The projected performance of an ideal DMT with a sampling rate of 1.024 MHz and 256-subchannel segmentation offers margin enhancement up to 3 dB over a quarter baud-spaced FSE-based 16-QAM signaling. However, more studies need to be performed to determine how well this analytically demonstrated enhancement can be achieved with a non-ideal DMT transceiver. For example, more sophisticated analyses and simulation studies which take into account effects such as finite length and finite precision filtering, intersymbol interference between subchannels, and adaptation residual error are in order.

6. Appendix: Margin in the Presence of FEXT&AWGN

Denote the transmit power by P_T and the load termination by R_L. The energy per block can be defined as: $P_T R_L$. Define M as the "number of

used sub-channels." To keep the transmit power constant, the energy per used sub-channel defined by α is: $\alpha \equiv \frac{1}{M}(P_T R_L)$. It is this energy per used sub-channel that determines the QAM constellation:

$$\alpha = \frac{1}{M}(P_T R_L) = \frac{L-1}{6} d^2 = E_{QAM} \quad \text{(A-1)}$$

Define η as the energy density per used-subchannel per Hz:

$$\eta = \frac{\alpha}{\Delta f} \ \ energy / Hz / sub-channel\ ,\ \Delta f = \frac{1}{T_{Symbol}} \quad \text{(A-2)}$$

Define the SNR/sub-channel as:

$$SNR_{i,M-DMT} = \frac{|H_i|^2 \eta}{\sigma_i^2} = \frac{|H_i|^2}{\sigma_i^2} \frac{(P_T R_L)}{M(\Delta f)} \quad \text{(A-3)}$$

where H_i is the loop transfer function at center frequency f_i, $\sigma_i^2 = \sigma_{i-FEXT}^2 + \sigma_{i-AWGN}^2$, $\sigma_{i-FEXT}^2 = \eta\, k_{FEXT}\, l\, |H_i|^2 f_i^2$, and $\sigma_{i-AWGN}^2 = 2\,\sigma_{AWGN}^2$. The factor of 2 in the previous expression accommodates white noise per 2-dimensional QAM symbol per sub-channel. Therefore equation (A-3) can be written as:

$$SNR_{i,M-DMT} = \left\{ k_{FEXT}\, l \left[f_i^2 + \frac{2\,\sigma_{AWGN}^2}{\frac{1}{M}\frac{(P_T R_L)}{\Delta f} k_{FEXT}\, l\, |H_i|^2} \right] \right\}^{-1} \quad \text{(A-4)}$$

Define the parameter β as:

$$\beta \equiv \frac{2\,\sigma_{AWGN}^2(\Delta f)}{k_{FEXT}\, l\, (P_T R_L)} \quad \text{(A-5)}$$

Thus, equation (A-4) can be expressed as:

$$SNR_{i,M-DMT} = \frac{1}{k_{FEXT}\, l} \left[f_i^2 + \frac{M\beta}{|H_i|^2} \right]^{-1} \quad \text{(A-6)}$$

The overall system $\overline{SNR}_{DMT}$ can be approximated by the geometric mean of the sub-channel SNRs defined by:[9]

$$\overline{SNR}_{DMT} = \frac{1}{k_{FEXT}\, l} \left[\prod_{j=1}^{M} \frac{1}{\left[f^j{}_i^2 + \frac{M\beta}{|H^j{}_i|^2} \right]} \right]^{\frac{1}{M}} \quad \text{(A-7)}$$

where $f^j{}_i$ and $|H^j{}_i|^2$ are corresponding frequency and insertion loss for $SNR^j{}_{i,M-DMT}$, and $SNR^j{}_{i,M-DMT}$ for $j = 1,2,\cdots,M$ are the M largest SNRs for a given M within a N sub-channels (i.e., i=1,2,...,N) ordered such that:

$$SNR^1{}_{i,M-DMT} > SNR^2{}_{i,M-DMT} > SNR^3{}_{i,M-DMT} > \cdots > SNR^M{}_{i,M-DMT} \quad \text{(A-8)}$$

Finally, the margin is calculated by:

$$\Delta_{DMT-margin} = -10\log_{10}\left[k_{FEXT} l \right] - 10\log_{10}\left[2^{b_{DMT}/M} - 1 \right] - \quad \text{(A-9)}$$

$$\frac{10}{M} \sum_{j=1}^{M} \log_{10}\left[f^j{}_i^2 + \frac{M\beta}{|H^j{}_i|^2} \right] - 9.8 \quad dB$$

REFERENCES

1. "Integrated Services Digital Network (ISDN)-Basic Access Interface," ANSI-T1.601, 1991.
2. "Generic Requirements for High-Bit-Rate Digital Subscriber Lines," Bellcore TA-NWT-001210, Issue 1, October 1991.
3. K. Sistanizadeh, "Performance Evaluation of 16/64-QAM ADSL Transceivers in the Presence of Self-FEXT," T1E1.4/91-117.
4. M. Sorbara, J. J. Werner, and N. A. Zervos, "Carrierless AM/PM," T1E1.4/90-154.
5. P.S. Chow, et al., "Preliminary Feasibility Study of a Multi-Carrier Transmission System for the Proposed ADSL Data Service," T1E1.4/90-211.
6. K. Sistanizadeh, "Proposed Canonical Loops for ADSL and their Loss Characteristics," T1E1.4/91-116.
7. J. Cioffi, et al., "A Comparison of Multi-Carrier and Single-Carrier Modulation for ADSL," T1E1.4/91-123.
8. P. S. Chow, et al., "Performance of Multicarrier with DSL Impulse Noise," T1E1.4/91-159.
9. J. M. Cioffi, "A Multicarrier Primer," T1E1.4/91-157.
10. K. Sistanizadeh, "Analysis and Performance Evaluation Studies of HDSL using QAM and PAM with Ideal DFE within a CSA," Proceedings of IEEE GLOBECOM'90 Conference, pp.1172-1176.
11. *Digital Communications*, J. G. Proakis, Second Edition, McGraw-Hill Book Company.
12. **Information Theory and Reliable Communication,** Chapter 8, R. G. Gallager, John Wiley & Sons, Inc., 1968.
13. Bellcore Database for 1983 Loop Survey.

Loop #	Margin dB
1	8.7
2	11.8
3	12.4
4	16.5
6	14.9
12-kft,24AWG	25.5
18-kft,24-AWG	19.8
9-kft,26-AWG	26.7

Table 1. DMT Margins with No Sub-Channel Exclusion

	16-QAM Margin dB			DMT Margin dB			Margin Enhancement dB		
	Guardband kHz			Excluded Sub-Channels Number			Excluded Sub-Channels Number		
Loop	20 kHz	50 kHz	100 kHz	1-10	1-25	1-50	1-10	1-25	1-50
1	2.7	0.6	-4.6	5.3	1.7	-3.5	2.6	1.1	1.1
2	8.2	4.0	-2.4	8.5	4.9	0.7	0.3	0.9	3.1
3	7.6	5.3	-1.6	8.9	4.9	0.0	1.3	-0.4	1.6
4	11.2	9.9	6.5	13.8	10.9	6.5	2.6	1.0	0.0
6	7.6	5.5	0.8	11.3	6.6	-0.7	3.7	1.1	-1.5
12kft,24	23.5	21.2	19.1	24.0	22.4	19.7	0.5	1.2	0.6
18kft,24	15.5	13.7	10.6	17.5	14.9	11.0	2.0	1.2	0.4
9kft,26	22.7	22.0	20.6	25.3	23.5	20.9	2.6	1.5	0.3

Table 2. 16-QAM and DMT Margins

Figure 1. Channel Spectrum Decomposition to Sub-Channel Spectra

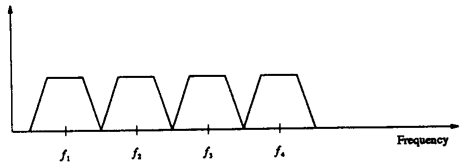

Figure 2. Transmit Energy Spectral Density

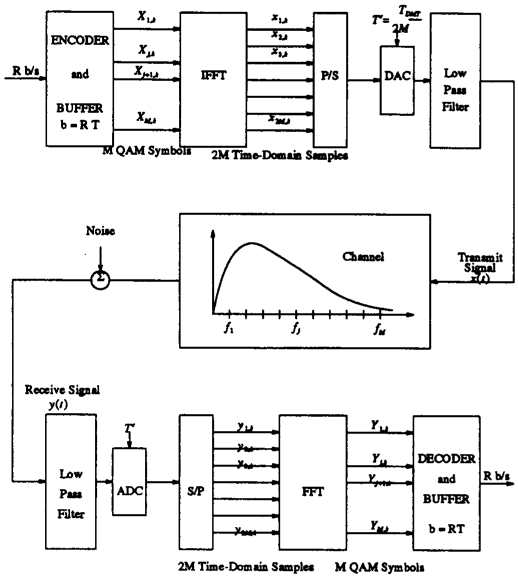

Figure 3. *DMT Transceiver Block Diagram*

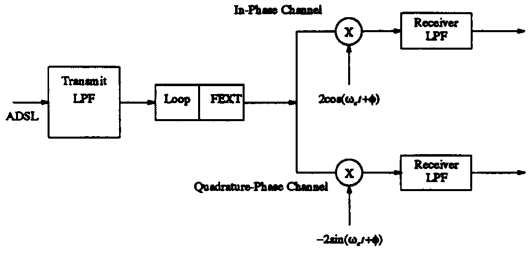

Figure 6. FEXT simulation model

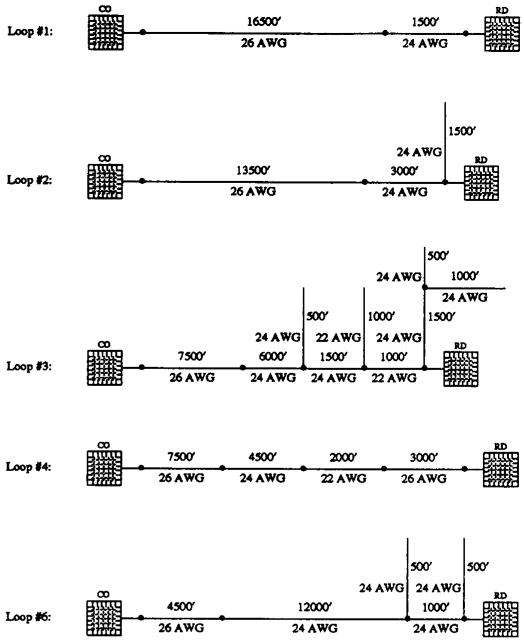

Note: 1) AWG means American Wire Gauge
2) Distances are in feet (′): 1000′ = .3048 km

Figure 5. Configuration of Test Loops

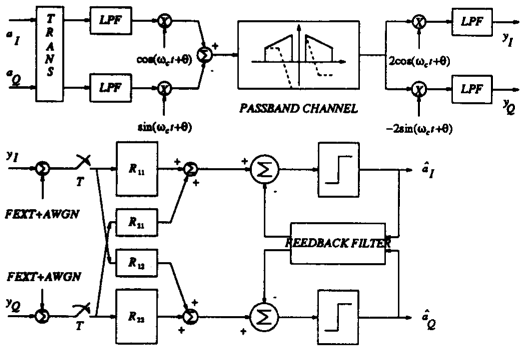

Figure 4. *QAM Transceiver Block Diagram*